
Physicochemical properties of aqueous core hydrogel capsules

Leslie Rolland,^a Enric Santanach-Carreras,^{b,‡} Thomas Delmas,^b Jérôme Bibette,^a and Nicolas Bremond^{*a}

Received Xth XXXXXXXXXXXX 20XX, Accepted Xth XXXXXXXXXXXX 20XX

First published on the web Xth XXXXXXXXXXXX 200X

DOI: 10.1039/b000000x

Capsules having a thin alginate hydrogel membrane and an aqueous core can be obtained by a process that involves a co-extrusion step in air followed by a sol-gel transition of the shell after immersion into a gelling bath. The possibility to encapsulate cells that further grow in these biocompatible compartments, and thus offer a versatile tool for cell culture, led us to investigate the physicochemical properties of the capsules. A cut-off pore size of the semi-permeable membrane is extrapolated from the release of polymers out of the capsule. When polymers can not diffuse through the membrane, the osmotic pressure mismatch between the core and the surrounding medium triggers an inflation of the capsule. The swelling may reach a steady state that allows to determine elastic features of the hydrogel shell. On the other hand, the capsule membrane may rupture and then contracts. From this stress-relaxation process, a critical deformation of the hydrogel shell above which plasticity occurs can be deduced. Finally, thanks to the physical nature of the hydrogel, the core content can be released by dissolving the membrane with the help of small electrolytes. The shell life is shown to vary inversely with the ionic strength of the solution.

1 Introduction

The compartmentalization of replicating molecules in cells is recognized to be the first evolutionary transition¹ that allows to link genotype (a nucleic acid that can be replicated) and phenotype (a functional trait). For instance, this feature has been exploited for the selection of enzymes by artificial compartmentalization in aqueous emulsion microdroplets². More recent works have also demonstrated the possibility to elaborate cell mimics from phospholipids vesicles where diblock copolymers are used as the elementary building block of the membrane³. The main difference is that the lipid bilayer is decorated with pumps or channels to ensure molecular exchange through the membrane, as it may occur in living cells⁴. Besides such compartment having a self-assembled membrane, other strategies to create liquid-core capsules which allow to compartmentalize molecules, particles or cells have been elaborated and find numerous applications from food industry⁵, water purification⁶, pharmaceuticals⁷ to cell encapsulation⁸. Most of the fabrication processes rely first on the formation of liquid droplets, either from an emulsification process or an atomization one. Then, among other methods, the solid shell is created by interfacial phase inversion⁹, inter-

nal phase separation^{10,11}, solvent evaporation of double emulsions¹², deposition of polyelectrolytes layers on a gelled core that is further liquified^{13,14} or by diffusion of the gelling agent either towards the core of the drop containing the polymers¹⁵ or from the core itself embedded in a polymer solution¹⁶.

Recently, we proposed a process for making capsules having a thin alginate hydrogel membrane and an aqueous core¹⁷. The method relies on a co-extrusion step in air followed by a sol-gel transition of the shell in a gelling bath and does not require the use of any solvent. It is thus a promising tool for cell culture, as demonstrated for micro-organisms¹⁷ and for the formation of mammalian cell aggregates, namely spheroids¹⁸.

Alginates, polysaccharides extracted from brown algae, have long being recognized as adequate biomaterials for biotechnology applications, from cell culture to tissue engineering, since they are biocompatible polymers that easily turn into gel with adaptable properties^{19,20}. Their chemical structure corresponds to a linear unbranched copolymers that contain homopolymeric blocks of (1→4)-linked β -D-mannuronic acid (M) and α -L-guluronic acid (G) as well as alternative sequence of M and G monomers. A sol-gel transition is triggered in presence of divalent cations like Ca^{2+} . The hydrogel network reticulation is provided by junction zones constituted of interchain G-blocks bound with divalent cations in a structure named "egg-box"^{21,22}. Recently, mixed junctions between G and MG blocks have been revealed²³. An important feature of the alginate hydrogel is the physical origin of the cross-links involving electrostatic and van der Waals forces and hydrogen bonds²⁴. The non-covalent nature of the cross-links allows rearrangement of the network *via* unbind-

^a Address, Laboratoire Colloïdes et Matériaux Divisés, from the Institute of Chemistry, Biology and Innovation (CBI) - ESPCI ParisTech / CNRS-UMR8231 / PSL* Research University, 10 rue Vauquelin 75231 Paris Cedex - France; E-mail: Nicolas.Bremond@espci.fr

^b Address, CAPSUM, Heliopolis, 3 allée des Maraîchers 13013 Marseille - France.

[‡] Present address: TOTAL S.A., Pôle d'Etudes et de Recherche de Lacq BP47 - 64170 Lacq - France

ing/binding events which can be induced by thermal fluctuations, residual internal stresses during gelation or under imposed stress or strain²⁵⁻²⁷. Moreover, since a small amount of polymers, of the order of 1 wt%, is used for making alginate hydrogel, the final material possesses a rather large permeability since cells can be immobilized while nutrients, like glucose, or compound excreted by the cells, like hormones can diffuse out²⁸. This retention and release feature of alginate hydrogels makes them a good carrier for drug release applications²⁹.

In this article, we probe the physicochemical properties of aqueous core capsules having a thin hydrogel membrane created by an original process. To do so, the capsules are exposed to various compositions of the core solution as well as the outer medium. First, the permeability features of the membrane are characterized by monitoring the release kinetic of small solutes and polymers of various sizes. Then, the response of the capsule subjected to an osmotic stress, induced by encapsulating polymers that can not diffuse through the hydrogel, is investigated. Finally, the disruption of the hydrogel shell *via* an ion exchange mechanism is explored.

2 Materials and methods

Chemicals. Sodium alginate Protanal LF200s, provided by FMC Biopolymer, is composed of about 70 % of guluronic acid and has an average molecular weight of 3×10^5 g/mol. Dextran, poly(ethylene) oxide (PEO), glucose, trisodium citrate, calcium chloride, potassium chloride, lithium chloride, sodium dodecyl sulfate (SDS) and Tween 20 were all purchased from Sigma Aldrich and used without any further purification. All solutions are made by using ultra pure water (Milli-Q).

Capsule fabrication. The capsules are formed by a co-extrusion technique previously reported¹⁷. Briefly, a compound drop having an aqueous core and an alginate solution shell is created at the end of a double concentric needle in a dripping regime. The shell turns into gel once the compound drop falls in a calcium chloride bath. Surfactants in the alginate solution, SDS, and in the gelling bath, Tween 20, are added for allowing the creation of thin hydrogel membrane¹⁷. The outer radius of the injector is 1.5 mm and the corresponding drop radius R is 1.73 mm. The average shell thickness h is controlled by the flow rate ratio $r_q = q_i/q_o$ between the inner one q_i and the outer one q_o , i.e. $h = R(1 - (r_q/(1 + r_q))^{1/3})$. The flow of both aqueous phases are driven by syringe pumps (PHD 2000, Harvard Apparatus). Flow rate ratio varies between 5 and 12 leading to an average membrane thickness lying between 45 μm to 100 μm and a ratio h/R ranging from 0.026 to 0.06. The capsules are left 30 s in the gelling bath containing 10 wt% of calcium chloride, then rinsed with wa-

ter, the excess of water around the capsule being soaked up with a tissue, and finally ready for further tests.

Release experiments. The core phase is a solution of glucose or dextran with $M_w = 2 \times 10^4$ g/mol at a concentration of 0.1 g/mL, or dextran with $M_w = 2 \times 10^6$ g/mol at a concentration of 0.075 g/mL. The hydrogel shell is made with 2 wt% of alginate and with 10 mM of SDS. The flow rate ratio is 10 which leads to an average membrane thickness of 50 μm . Following their formation, 10 capsules are stored in a 1 mL core solution. After 1 hour, 0.95 mL are pipetted off the container and 1 mL of milliQ water is added. The concentration of glucose or dextran $C_o(t)$ is then measured over time in the external bath under constant stirring. The outer concentration is evaluated from the index of refraction measured with a refractometer (Abbemat WR, Anton Paar) having a precision of 3.15×10^{-4} g/mL. The polymers features are characterized by static and dynamic light scattering technique (CGS-3, ALV-GmbH).

Swelling experiments. A capsule with a dextran or PEO core solution and made of various alginate concentrations is first dropped in a glass cuvette filled with pure water. The time of immersion defines the time $t = 0$ of the experiment. The evolution of the capsule undergoing an osmotic stress is then recorded with a CCD camera coupled with a backlight system. The capsule size is measured by using an image processing program developed with MATLAB.

Bursting experiments. The hydrogel membrane is here composed of 2 wt% of alginate and the average shell thickness is close to 50 μm , corresponding to $h/R = 0.03$. The capsules are immersed alone in 50 mL of an electrolyte solution made from NaCl, KCl, LiCl or trisodium citrate. The lifetime of the capsule membrane is then estimated by the naked eye with the help of a stopwatch. A small amount, 0.1 wt%, of natural rubber latex is added into the core solution for visualizing the time of bursting that leads to a sudden release of the colloidal particles. The bursting time t_b is averaged over 10 experiments.

3 Results and discussion

3.1 Transport through the membrane

The hydrogel is by definition mainly composed of water and thus is a highly porous material. The network mesh size can be assessed by rheological characterization, NMR relaxometry or TEM micrograph analysis³⁰. This mesh size, that depends on alginate concentration and G/M ratio, impacts on the mechanical properties of the hydrogel as well as the diffusion properties of solutes³¹. Another characteristic length scale, the maximal pore size, can be evaluated by an inverse steric exclusion chromatography approach³². This cut-off size

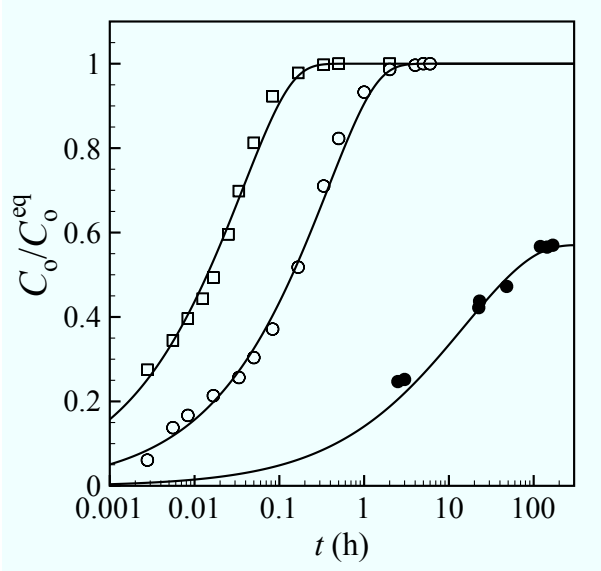


Fig. 1 Release kinetics of (□) glucose, (○) dextran with $M_w = 2 \cdot 10^4$ g/mol, and (●) dextran with $M_w = 2 \cdot 10^6$ g/mol from a capsule made with an alginate concentration of 2 wt%. The outer concentration C_o of either glucose or dextran is measured by refractometry and normalized by the equilibrium concentration C_o^{eq} estimated for a fully permeable hydrogel membrane.

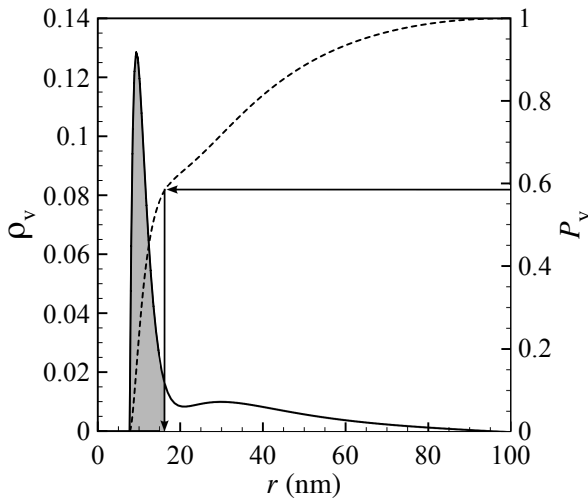


Fig. 2 Volume probability density function ρ_v as a function of coil size r of dextran with $M_w = 2 \cdot 10^6$ g/mol measured by dynamic light scattering as well as the corresponding volume cumulative density function P_v . The grey area corresponds to the polymer mass proportion that escapes from the capsule and that finally defines a cut-off radius of the membrane of 16 nm as indicated by the arrow.

is an important parameter to know for encapsulation applications. Moreover, the structural properties of a hydrogel depend on the way the sol-gel transition is induced and can be inhomogeneous on millimeter scale³³. The porosity of the hydrogel can be characterized by monitoring the release of solutes from the core, that is either gelled or liquid, to the surrounding medium^{34,35}. Here, we use a liquid core composed of solutions of glucose and dextran having different molecular weights. The kinetic release of small solutes as compared to the characteristic pore size can be analytically described by solving the diffusion equation in a spherical geometry³⁶. For homogeneous porous spheres and if the surrounding concentration of solutes is assumed to be homogeneous, when the dispersion of spheres is stirred as it is the case here, the outer concentration C_o is given by

$$\frac{C_o(t)}{C_o^{eq}} = 1 - \sum_{k=1}^{\infty} \frac{6\alpha(1+\alpha)}{9+9\alpha+\alpha^2 q_k^2} \exp\left(\frac{-Dq_k^2 t}{R^2}\right) \quad (1)$$

where C_o^{eq} is the expected outer concentration that depends on the initial inner concentration C_i^0 and α which is the ratio between the volume of the continuous phase and the sphere volume, i.e. $\alpha = C_i^0/C_o^{eq} - 1$ by assuming a partition coefficient between the hydrogel and water equal to 1, R is the sphere radius, D is the diffusion coefficient of the solutes in the hydrogel and q_k is the k th positive roots of

$$\tan q_k = \frac{3q_k}{3 + \alpha q_k^2} \quad (2)$$

As reported in Fig. 1, the equilibrium concentration of glucose in the surrounding medium is reached after about 0.1 h. Assuming that the concentration profile built in the sphere and that leads to Eq. 1 holds for a liquid core capsule case, a diffusion coefficient D of glucose equal to $1.4 \cdot 10^{-9} \text{ m}^2 \cdot \text{s}^{-1}$ is deduced. This value is about two times larger than the one measured in an infinitely dilute solution of glucose at 25°C which is $6.75 \cdot 10^{-10} \text{ m}^2 \cdot \text{s}^{-1}$ ³⁷. The release dynamics of glucose is thus observed to be sped up by the motion of the capsule under stirring. The rotation and collision of the capsules induce a momentum transfer into the liquid core and thus modify the purely diffusive mechanism that results in Eq. 1. When a branched polymer of glucose, dextran, having a molecular weight M_w of $2 \cdot 10^4$ g/mol is mixed into the core solution the characteristic time of the release kinetics is observed to be around 1 h, i.e. ten times slower than glucose (Fig. 1). The corresponding diffusion coefficient extrapolated from the release kinetics by using Eq. 1 is $1.4 \cdot 10^{-10} \text{ m}^2 \cdot \text{s}^{-1}$. This is coherent with dynamic light scattering measurements of dextran solutions where the diffusion coefficient D is shown to vary like $M_w^{-\nu}$ where $\nu \sim 0.44$ ³⁸. Therefore, both glucose and dextran with M_w of $2 \cdot 10^4$ g/mol diffuse freely through the hydrogel membrane.

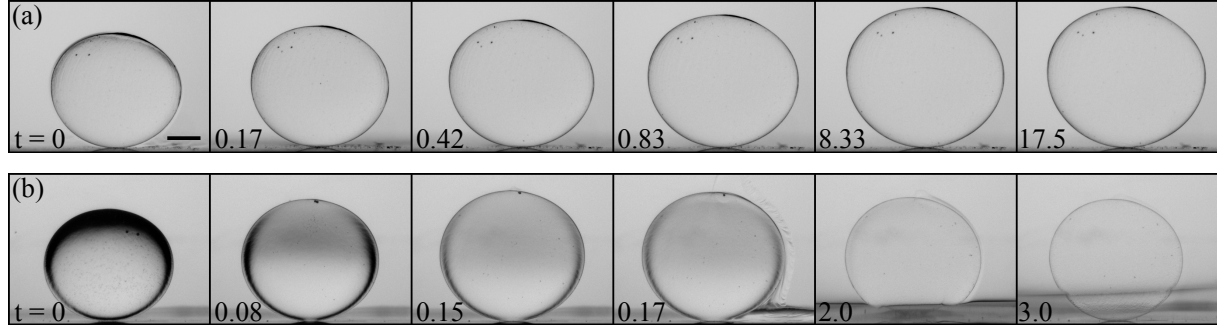


Fig. 3 (a) Time sequence of a capsule under osmotic stress that swells and whose deformation saturates. Here $C_{alg} = 3$ wt%, $h/R = 0.031$, and the core is composed of a dextran solution at $C_0 = 100$ g.l⁻¹. (b) Time sequence of a capsule that initially expands and then contracts after the membrane ruptures at $t = 0.17$ h. Here $C_{alg} = 2$ wt%, $h/R = 0.031$, $C_0 = 200$ g.l⁻¹. The dextran used for the experiments has a molecular weight of 2×10^6 g/mol. Time is indicated in hour, and the scale bar corresponds to 1 mm.

On the other hand, if a much larger dextran is used, with $M_w = 2 \times 10^6$ g/mol, only 58 % of the expected mass is recovered after 100 h as shown in Fig. 1. The extrapolated coefficient of diffusion is 3×10^{-12} m².s⁻¹, which is more than one order of magnitude smaller than expected. The diffusion of dextran having such a size is now hindered by the alginate network. Moreover, part of the polymers are kept trapped inside the capsule core. As reported in Fig. 2, there exists a widespread size distribution of such natural macromolecules. A cut-off pore size r^* of the membrane can then be deduced from the integration of the volume probability density function ρ_v and the maximum concentration C_o^{\max} reached by the outer solution

$$\frac{C_o^{\max}}{C_o^{\text{eq}}} = \int_0^{r^*} \rho_v dr \quad (3)$$

For a hydrogel membrane made with a 2 wt% alginate solution, a cut-off pore size r^* of 16 nm is estimated. This value is in a good agreement with previous estimations based on different techniques³⁰. We then wonder how the capsule shape is affected when a high molecular weight polymer is entrapped into the core.

3.2 Capsule under osmotic stress

When an aqueous core capsule that contains solutes is immersed into another aqueous medium with a different solutes concentration, the osmolality mismatch drives the fluxes of solvent, here water, and solutes through the membrane. For large molecules, and thus for a low diffusion coefficient, water molecules diffuse faster for homogenizing the chemical potential of water. This flux induces an inflation of the capsule for a hypotonic condition. If the solutes can diffuse through the hydrogel membrane, like the dextran with $M_w = 2 \times 10^4$ g/mol, the transient osmotic pressure then relaxes and so does

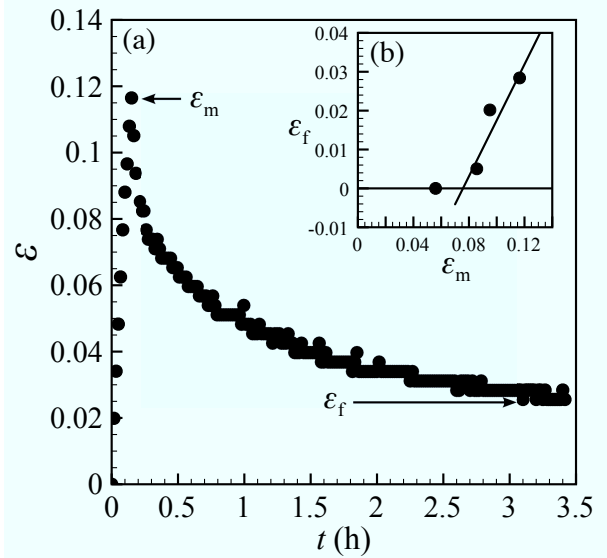


Fig. 4 (a) Time evolution of the strain ϵ estimated from the capsule width W , i.e. $\epsilon = W/W_0 - 1$, for a capsule that bursts. (b) Final strain ϵ_f as a function of the maximal strain ϵ_m before capsule bursting. The continuous lines are used to extrapolate a critical strain equal to 0.076 beyond which plastic deformations occur.

the capsule size. On the other hand, for large macromolecules that are kept trapped inside the core, the capsule swelling saturates. An example of such a phenomenon, obtained with a solution of dextran with $M_w = 2 \times 10^6$ g/mol at an initial concentration C_0 of 100 g.L^{-1} , is reported in Fig. 3 (a). If the capsule membrane is thinner or if a higher osmotic pressure is imposed, the capsule membrane may rupture while it inflates and then contracts as shown in Fig. 3 (b). Two main properties of the hydrogel membrane can be inferred from these experiments when the corresponding strain ε is analyzed. The strain is defined from the capsules width W , i.e. $\varepsilon = W/W_0 - 1$ where W_0 is the initial width. We stress that since the capsules are not perfect spheres nor perfect spheroids, we study the evolution of the maximal characteristic length, i.e. the width, that lies in the equatorial plan of the compound drop which is initially perpendicular to the gravity direction before the impact into the gelling bath.

First, as observed in the bursting case (Fig. 4 (a)), the strain reaches a maximum value ε_m and relaxes towards a non-zero final value ε_f . This indicates irreversible deformations undergone by the hydrogel. As reported in Fig. 4 (b), plastic deformations are present as soon as the strain is larger than 0.076. Then, the final strain varies linearly with the maximal strain like $\varepsilon_f = -0.055 + 0.72 \varepsilon_m$.

Second, if the membrane does not rupture, the maximum size attained by the capsule gives us information on elastic properties of the hydrogel shell if the amount of polymer trapped inside the capsule, and thus the osmotic pressure, is known. This is the case when a PEO with $M_w = 10^6$ g/mol is used since we do not measure any release of the polymer out of the capsule core. As reported in Fig. 5, for a membrane made with $C_{alg} = 3 \text{ wt}\%$, the maximal strain goes from 0.036 to 0.08 when the average shell thickness to capsule size ratio is tuned from 0.06 to 0.026, respectively. Therefore, ε_m is inversely proportional to h/R . Then, if the alginate content is reduced to 2 wt%, ε_m jumps to 0.12 when $h/R = 0.026$. Moreover, as shown in Fig. 6 (a), ε_m is an increasing function of the entrapped polymer concentration and thus of the osmotic pressure Π . Let us consider the capsule as a balloon of constant shell thickness under a pressure Π . Since the shell thickness h to capsule size R ratio is weak, the corresponding stretching stress σ along the shell can be considered as homogeneous and equal to $2\Pi R/h$ ^{39,40}. For small deformation, the strain should be proportional to σ and inversely proportional to the Young modulus E . One can thus anticipate the results reported in Fig. 5 and Fig. 6(a) where, for a given osmotic pressure difference, the strain decreases when the shell thickness is reduced or when the amount of alginate is lowered since E is an increasing function of C_{alg} .

As detailed elsewhere¹⁸, the final strain ε_m gives access to an estimation of the elastic modulus E of the hydrogel by balancing the stored elastic energy and the work done by the os-

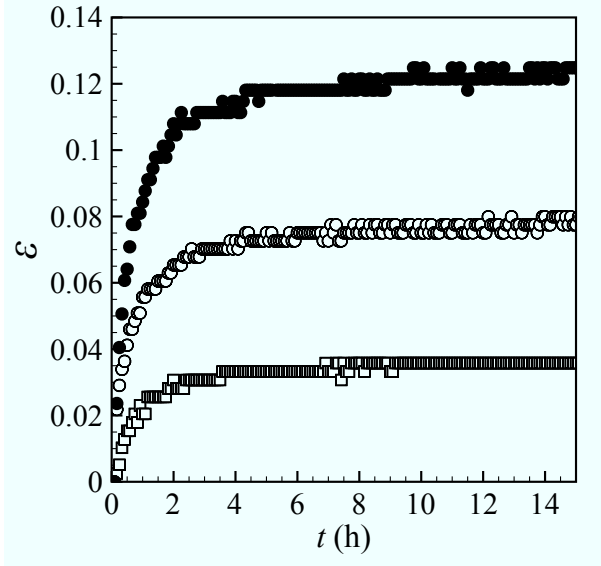


Fig. 5 Time evolution of the strain ε for stable capsules having different membrane composition and thickness: (□) $C_{alg} = 3 \text{ wt}\%$, $h/R = 0.06$, (○) $C_{alg} = 3 \text{ wt}\%$, $h/R = 0.026$, and (●) $C_{alg} = 2 \text{ wt}\%$, $h/R = 0.026$. The polymers used is PEO at 2 wt%.

motric pressure difference. The osmotic pressure depends on polymer concentration C , i.e. $\Pi = \mathcal{R}T \left(\frac{1}{M_w} C + A_2 C^2 \right)$ where Π is in Pa, C is expressed in mol.m^{-3} , A_2 is the second virial coefficient and \mathcal{R} the gas constant. For a PEO with an average molecular weight M_w of 10^6 g/mol this term is equal to $1.2 \times 10^{-3} \text{ m}^3 \cdot \text{mol.kg}^{-2}$ as measured by static light diffusion technique⁴¹. By expressing the concentration in g.l^{-1} , the osmotic pressure finally writes $\Pi = \alpha C + \beta C^2$ with $\alpha = 2.48 \text{ Pa.g}^{-1}$ and $\beta = 2.97 \text{ Pa.g}^{-2}$,¹² at $T = 298 \text{ K}$. By taking into account dilution of the inner polymer solution and thinning of the shell during inflation and by considering an incompressible material, i.e. having a Poisson ratio ν equal to 1/2, the maximum strain at equilibrium when the outer medium is free of polymer is given by¹⁸

$$\varepsilon_m = \frac{\Pi_0}{\Pi_c - 4E(h_0/R_0)} \quad (4)$$

where the parameters with the subscript 0 correspond to their initial value before swelling and $\Pi_c = \Pi_0 - 3\beta C_0^2$. The Young modulus can thus be inferred by measuring ε_m . An estimation of E is reported in Fig. 6 (b) for $C_{alg} = 2 \text{ wt}\%$ as a function of ε_m . The elastic modulus is constant and equal to $60 \pm 2 \text{ kPa}$ for maximal strain smaller than 0.08 and then decreases when ε_m increases. The manifestation of this apparent strain softening behavior corresponds to the elastic-plastic transition observed from the strain relaxation experiments reported in Fig. 4. In addition, for a higher alginate content equal to 3 wt%, the corresponding elastic modulus is evalu-

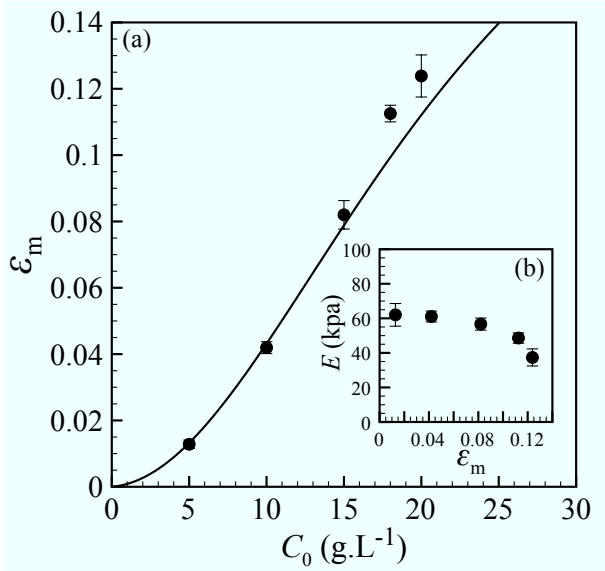


Fig. 6 (a) Evolution of the maximal strain ϵ_m of stable capsules as a function of the initial PEO concentration C_0 . The continuous line represents Eq. 4 with an elastic modulus E equal to 60 kPa. (b) Elastic modulus versus maximal strain showing a strain softening behaviour.

ated to be 120 ± 10 kPa. The estimated Young modulus is in a good agreement with previous studies based on classical characterization techniques on a similar alginate^{42,43}. However, we stress that here these values have been extrapolated by assuming a homogeneous shell thickness which is not exact for the present capsules made in a dripping regime but more realistic from those fabricated *via* the fragmentation of a compound liquid jet¹⁸.

3.3 Shell dissolution with electrolytes

The complexation of alginate with divalent cations lead to a three-dimensional percolated network once the alginate concentration C_{alg} is roughly above 0.8 wt%. Moreover, the sol-gel transition becomes independent on the cation concentration for C_{alg} larger than 1.2 wt%⁴⁴. In our case, the critical concentration of calcium chloride is found to be 10^2 mol/l. Interestingly, when a hydrogel capsule is let in a large volume of pure water, the membrane does not dissolve. This indicates a high energy barrier to overcome for the calcium ion to escape the "egg-box" trap. Indeed, the electrostatic energy between the ion Ca^{2+} and its nearest neighbors O atoms is around $12 k_B T$ ⁴⁵ and the corresponding energy for disassembling chain pairs of calcium-gulonate oligomers has been evaluated around $200 k_B T$ for $T = 298$ K²⁴. Once monovalent ions are added, the gel swells⁴⁶ and softens⁴⁷ because of ion displacement that has been suggested to result from a steric

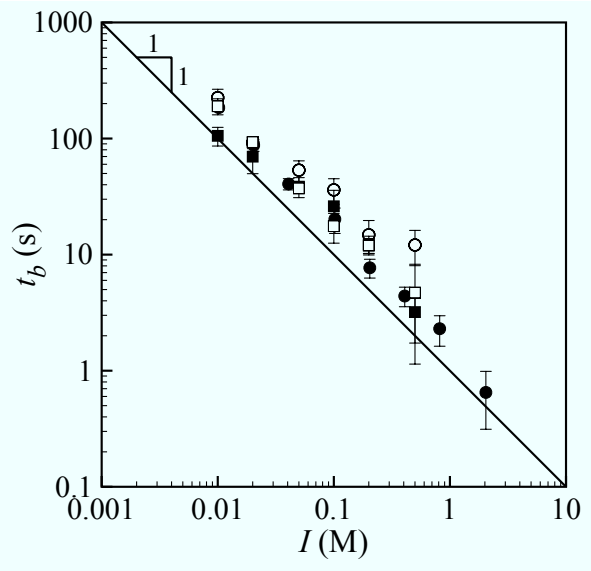


Fig. 7 Bursting time t_b of capsules when immersed in an electrolyte solution as a function of the ionic strength I of (●) trisodium citrate, (○) sodium chloride, (■) potassium chloride and (□) lithium chloride solutions. The alginate concentration is 2 wt% and the average membrane thickness is $50 \mu\text{m}$.

process²⁵. However, we stress that the thermodynamic equilibrium of the hydrogel is not changed in presence of monovalent ions since the critical concentration of Ca^{2+} for the sol-gel transition is unaltered. On the other hand, the transition is modified if a chelating agent of the divalent ions is added to the solution.

We investigate the stability of capsules immersed in electrolytes solutions free of calcium but containing various monovalent ions. A chelant of calcium, trisodium citrate, is also used. The alginate hydrogel membrane is observed to burst after a time t_b spent in the electrolyte solution. The bursting time is a decreasing function of the salt concentration and, as reported in Fig. 7, it is only a function of the ionic strength I of the solution. Moreover, t_b is inversely proportional to I , which is a signature of a first order reaction. Within the experimental accuracy of the measurements, we do not observe any clear dependence of the capsule lifetime on the size of the cations Li^+ , Na^+ and K^+ . We note that diffusion of the cations through the gel is not limiting for such lifetimes since the diffusive length scale, i.e. $(Dt_b)^{1/2}$ where the coefficient of diffusion is around $10^{-9} \text{ m}^2 \cdot \text{s}^{-1}$, is of the order of the shell thickness for $t_b \sim 1$ s. Finally, adding a chelating agent of Ca^{2+} or working at a large dilution lead to the same dissolution kinetics of the hydrogel membrane.

4 Conclusion

This article reports an investigation on the physicochemical properties of aqueous core capsules having a thin membrane. The capsule shell is an hydrogel composed of alginate physically cross-linked by divalent cations. First, a cut-off pore size of the semi-permeable membrane is determined from the partial release from the capsule of polymers having a widespread size distribution. For a hydrogel membrane built with 2 wt% of alginate, this maximal pore size is estimated to be 16 nm. Then, knowing this characteristic size, high molecular weight polymers can be trapped inside the capsule core. Therefore, an osmotic pressure mismatch between the core and the surrounding can be imposed. Two mechanical tests of the hydrogel shell can then be conducted. The first one corresponds to a strain-relaxation process where first the capsule inflates under osmotic pressure and then deflates after the shell ruptures at one point. Depending on the maximal strain at which the shell breaks, the final strain may not relax to zero, meaning that the hydrogel undergoes irreversible deformations. The critical strain above which creeping of the material occurs is estimated at around 8 %. If now a lower amount of polymers is encapsulated, and thus for a weaker osmotic pressure, or if the shell thickness is increased or the alginate concentration is raised, then the capsule might be mechanically stable. In that case, the strain saturates to a maximal value that depends on the geometrical features of the capsule, h/R , the elastic modulus E of the material and the osmotic pressure linked to concentration of entrapped polymers. More precisely, under the assumption that the shell thickness is homogeneous and the material incompressible, and for low deformation, E is found to be around 60 kPa for $C_{alg} = 2$ wt% and jumps to 120 kPa for $C_{alg} = 3$ wt%. The dependence of E on polymer concentration that scales like C_{alg}^2 is a feature shared by other biopolymer gels⁴⁸. Finally, since we consider here a physical gel, the capsule content can be released by dissolving the membrane *via* an ion exchange mechanism. This is realized by immersing the capsules in aqueous solution containing monovalent ions. We observe that finally the lifetime of the hydrogel shell, when bursting occurs, is inversely proportional to the ionic strength of the solution.

As stated in the introduction, such a capsule having an aqueous core with a semi-permeable membrane composed by a biocompatible material and fabricated *via* a solvent free process offers a new tool for cell culture. Decreasing the capsule size in a controlled manner is necessary for widen its field of applications as already demonstrated for the formation and the growth of cancer cell spheroids under confinement¹⁸. Making smaller capsules requires to create and to break a submillimetric compound jet. This process implies the annular co-flow of phases having different viscoelastic properties, a situation that is potentially unstable^{49,50}, as well as as the fragmentation of

a stratified liquid jet under a capillary instability. Controlling such instabilities would guarantee a robust and efficient cell encapsulation method opening the way to high throughput applications.

References

- 1 E. Szathmary and J. M. Smith, *Nature* **374**(6519), 227 (1995).
- 2 D. S. Tawfik and A. D. Griffiths, *Nat. Biotechnol.* **16**(7), 652 (1998).
- 3 B. M. Discher, Y. Y. Won, D. S. Ege, J. C. M. Lee, F. S. Bates, D. E. Discher, and D. A. Hammer, *Science* **284**, 1143 (1999).
- 4 V. Noireaux and A. Libchaber, *Proc. Natl. Acad. Sci. USA* **101**(51), 17669 (2004).
- 5 A. Madene, M. Jacquot, J. Scher, and S. Desobry, *Int. J. Food Sci. Technol.* **41**(1), 1 (2006).
- 6 M. Whelehan, U. von Stockar, and I. W. Marison, *Water Res.* **44**(7), 2314 (2010).
- 7 C. E. Mora-Huertas, H. Fessi, and A. Elaissari, *Int. J. Pharm.* **385**(1-2), 113 (2010).
- 8 J. K. Park and H. N. Chang, *Biotechnol. Adv.* **18**(4), 303 (2000).
- 9 M. V. Sefton, R. M. Dawson, R. L. Broughton, J. Blynsniuk, and M. E. Sugamori, *Biotechnol. Bioeng.* **29**(9), 1135 (1987).
- 10 A. Loxley and B. Vincent, *J. Colloid Interface Sci.* **208**(1), 49 (1998).
- 11 R. Atkin, P. Davies, J. Hardy, and B. Vincent, *Macromolecules* **37**(21), 7979 (2004).
- 12 A. S. Utada, E. Lorenceau, D. R. Link, P. D. Kaplan, H. A. Stone, and D. A. Weitz, *Science* **308**(5721), 537 (2005).
- 13 E. Donath, G. B. Sukhorukov, F. Caruso, S. A. Davis, and H. Mohwald, *Angew. Chem., Int. Ed.* **37**(16), 2202 (1998).
- 14 V. Breguet, R. Gugerli, M. Perneti, U. von Stockar, and I. W. Marison, *Langmuir* **21**(21), 9764 (2005).
- 15 T. Wang, I. Lacik, M. Brissova, A. V. Anilkumar, A. Prokop, D. Hunkeler, R. Green, K. Shahrokhi, and A. C. Powers, *Nat. Biotechnol.* **15**(4), 358 (1997).
- 16 H. N. Chang, G. H. Seong, I. K. Yoo, J. K. Park, and J. H. Seo, *Biotechnol. Bioeng.* **51**(2), 157 (1996).
- 17 N. Bremond, E. Santanach-Carreras, L. Y. Chu, and J. Bibette, *Soft Matter* **6**(11), 2484 (2010).
- 18 K. Alessandri, B. R. Sarangi, V. V. Gurchenkov, B. Sinha, T. R. Kiessling, L. Fetter, F. Rico, S. Scheuring, C. Lamaze, A. Simon, et al., *Proc. Natl. Acad. Sci. USA* **110**(37), 14843 (2013).
- 19 O. Smidsrød and G. Skjåk-Bræk, *Trends Biotechnol.* **8**(0), 71 (1990).
- 20 A. D. Augst, H. J. Kong, and D. J. Mooney, *Macromol. Biosci.* **6**(8), 623 (2006).
- 21 G. T. Grant, E. R. Morris, D. A. Rees, P. J. Smith, and D. Thom, *FEBS Lett.* **32**(1), 195 (1973).
- 22 E. R. Morris, D. A. Rees, D. Thom, and J. Boyd, *Carbohydr. Res.* **66**(1), 145 (1978).
- 23 I. Donati, S. Holtan, Y. A. Morch, M. Borgogna, M. Dentini, and G. Skjåk-Bræk, *Biomacromolecules* **6**(2), 1031 (2005).
- 24 I. Braccini and S. Perez, *Biomacromolecules* **2**(4), 1089 (2001).
- 25 T. Baumberger and O. Ronsin, *Biomacromolecules* **11**(6), 1571 (2010).
- 26 D. Larobina and L. Cipelletti, *Soft Matter* **9**(42), 10005 (2013).
- 27 E. Secchi, T. Roversi, S. Buzzaccaro, L. Piazza, and R. Piazza, *Soft Matter* **9**(15), 3931 (2013).
- 28 F. Lim and A. Sun, *Science* **210**(4472), 908 (1980).
- 29 W. R. Gombotz and S. Wee, *Adv. Drug Delivery Rev.* **31**(3), 267 (1998).
- 30 G. Turco, I. Donati, M. Grassi, G. Marchioli, R. Lapasin, and S. Paoletti, *Biomacromolecules* **12**(4), 1272 (2011).
- 31 B. Amsden, *Macromolecules* **31**(23), 8382 (1998).

-
- 32 J. Klein, J. Stock, and K. D. Vorlop, *Eur. J. Appl. Microbiol. Biotechnol.* **18**(2), 86 (1983).
 - 33 G. Skjåk-Bræk, H. Grasdalen, and O. Smidsrød, *Carbohydr. Polym.* **10**(1), 31 (1989).
 - 34 H. Tanaka, M. Matsumura, and I. A. Veliky, *Biotechnol. Bioeng.* **26**(1), 53 (1984).
 - 35 R. H. Li, D. H. Altreuter, and F. T. Gentile, *Biotechnol. Bioeng.* **50**(4), 365 (1996).
 - 36 J. Crank, *The mathematics of diffusion* (Oxford University Press, 1975).
 - 37 J. K. Gladden and M. Dole, *J. Am. Chem. Soc.* **75**(16), 3900 (1953).
 - 38 E. Nordmeier, *J. Phys. Chem.* **97**(21), 5770 (1993).
 - 39 S. Timoshenko, S. Woinowsky-Krieger, *Theory of Plates and Shells* (McGraw-Hill, 1959).
 - 40 M. J. Mela, *Biophys. J.* **7**(1), 95 (1967).
 - 41 K. Devanand and J. C. Selser, *Macromolecules* **24**(22), 5943 (1991).
 - 42 K. I. Draget, G. S. Skák-Bræk, and O. Smidsrød, *Carbohydr. Polym.* **25**(1), 31 (1994).
 - 43 H. J. Kong, K. Y. Lee, and D. J. Mooney, *Polymer* **43**(23), 6239 (2002).
 - 44 Y. Y. Zhao, F. P. Hu, J. J. Evans, and M. T. Harris, *Chem. Eng. Sci.* **66**(5), 848 (2011).
 - 45 T. Baumberger and O. Ronsin, *J. Chem. Phys.* **130**(6), 061102 (2009).
 - 46 X. Wang and H. Garth Spencer, *Polymer* **39**(13), 2759 (1998).
 - 47 M. A. LeRoux, F. Guilak, and L. A. Setton, *J. Biomed. Mater. Res.* **47**(1), 46 (1999).
 - 48 A. Clark and S. Ross-Murphy, in *Advances in Polymer Science* (Springer Berlin Heidelberg, 1987), vol. 83, pp. 57–192.
 - 49 R. G. Larson, *Rheol. Acta* **31**(3), 213 (1992).
 - 50 R. Govindarajan and K. C. Sahu, *Annu. Rev. Fluid Mech.* **46**, 331 (2014).